Amplified Spontaneous Emission of Surface Plasmon Polaritons with Unusual Angle-Dependent Response

Yu-Hui Chen, Jiafang Li, Ming-Liang Ren, and Zhi-Yuan Li**

Surface plasmon polaritons (SPPs) have drawn much attention due to their subwavelength field confinement, strong field enhancement, and high sensitivity to environments.[1] However, the applications of SPPs have been largely hindered by the SPP energy dissipation in the metals. It has been shown that the ohmic loss of SPP can be compensated by the introduction of optical gain media,[2–8] and versatile configurations have been proposed with various gain media, such as optically pumped dye molecules,[2–4] optically pumped quantum dots,[6,7] and electrically pumped quantum wells.[8] However, many reports still focus on recognizing the existence of SPP amplification in systems, and due to limited and insufficient experimental observations, different and controversial points of view on novel concepts have arisen, e.g., surface plasmon amplification by stimulated radiation (spaser).[9] Meanwhile, how the gain affects the performance of SPP devices, whether there exists an optimal gain for a specific SPP system, and what happens if gain is over the SPP energy dissipation, are still not clear.

Based on a typical Kreschmann configuration, we have shown direct evidence of amplified spontaneous emission (ASE) of surface plasmon polaritons (ASE_{SPP}) at the interface of a silver film and a gain medium.[10] Here, by further carrying out the measurements, we report that with the increase of gain, the ASE_{SPP} undergoes an unusual angular response, i.e., the amplified SPP is decoupled to emit in a broadened angular range with increased pump intensity. Our theoretical studies have indicated that this unusual angular response can be attributed to the growing net gain in the structure when the pump intensity is increased.

Our experimental setup is based on a typical Kretschmann configuration. As shown in **Figure 1**a, the thickness of the silver film, the SiO_2 layer, and the poly(methyl methacrylate) (PMMA)/Rhodamine 6G (Rh6G) film is 55 nm, 5 nm, and 1.3 μm, respectively. A pulse (with 532 nm wavelength, ~5 ns duration, 0.5 Hz repetition rate, and polarization normal to the *xz* plane) is used to excite the Rh6G molecules from the PMMA film side. More detailed descriptions of the experiments can be found in the Experimental Section and literature.[10] After the pump pulse strikes at the PMMA/Rh6G film, the molecules are excited and re-radiate photons, which are then coupled to the SPP modes[4,11] that propagate along the interface of silver and PMMA/Rh6G. Such SPP modes are inherently leaky modes,[12,13] which are simultaneously decoupled into radiative waves by the prism at an angle that satisfies $\sqrt{\varepsilon_1}\sin\theta = \sqrt{\varepsilon_2\varepsilon_3/(\varepsilon_2 + \varepsilon_3)}$, where ε_i ($i = 1, 2, 3$) is the permittivity of the ith medium as marked in Figure 1a. As a result, the measured signal in far field is a function of wavelength λ and decoupled angle θ (θ is the angle measured inside the prism). Figure 1b shows the decoupled emission spectra of SPPs at several decoupling angles, which show that only those SPPs with frequencies satisfying $\sqrt{\varepsilon_1}\sin\theta = \sqrt{\varepsilon_2\varepsilon_3/(\varepsilon_2 + \varepsilon_3)}$ could emit into the prism at a specific angle θ. While in Figure 1c, the SPP emission intensity as a function of the decoupling angle, i.e., the angular distribution of SPP emission, is plotted for each specific wavelength. It can be seen that at each specific wavelength, the angular distribution curve shows a narrow peak with an FWHM (full width at half maximum) of 1–2°. Meanwhile, it is obvious that both the peak position and FWHM of the curves are wavelength-dependent. For example, the FWHM at 555.80 nm is narrower than that at 600.53 nm. As the pump intensity increases, an ASE_{SPP} peak arises and its position is independent on the decoupling angle (Figure 1d), similarly as reported in our previous work.[10]

Generally, it is expected that the introduction of gain will compensate the dissipation losses and therefore narrow down the SPP emission spectra, which have been confirmed in our experiments[10] and some other works.[7,14] In the same way, it is naturally expected that the introduced gain could also improve the performance in the angular response of the plasmonic system, i.e., narrow down the angular response of the SPP emission. However, we observed unusual effects. As plotted in **Figure 2**a,b, at some wavelengths, the angular distribution of the SPP emission shows nearly no change when increasing the pump intensity I_P from 0.54 to 1.91 mJ/cm^2. While at certain wavelength range, the FWHM is unusually broadened with increased pump intensity. For example, at the ASE_{SPP} peak wavelength 592.87 nm, the FWHM increases from 1.11° to 1.31° when I_P grows from 0.54 to 1.91 mJ/cm^2 (see Figure 2c). To find out the trend of the unusual angular broadening, the wavelength-dependent response of the angular FWHM on increased pump intensity is further illustrated in Figure 2d. It is worthwhile to point out two features.

Y. H. Chen, Dr. J. F. Li, M. L. Ren, Prof. Z. Y. Li
Laboratory of Optical Physics
Institute of Physics
Chinese Academy of Science
Beijing 100190, China
E-mail: jiafangli@aphy.iphy.ac.cn;
lizy@aphy.iphy.ac.cn

DOI: 10.1002/smll.201101806

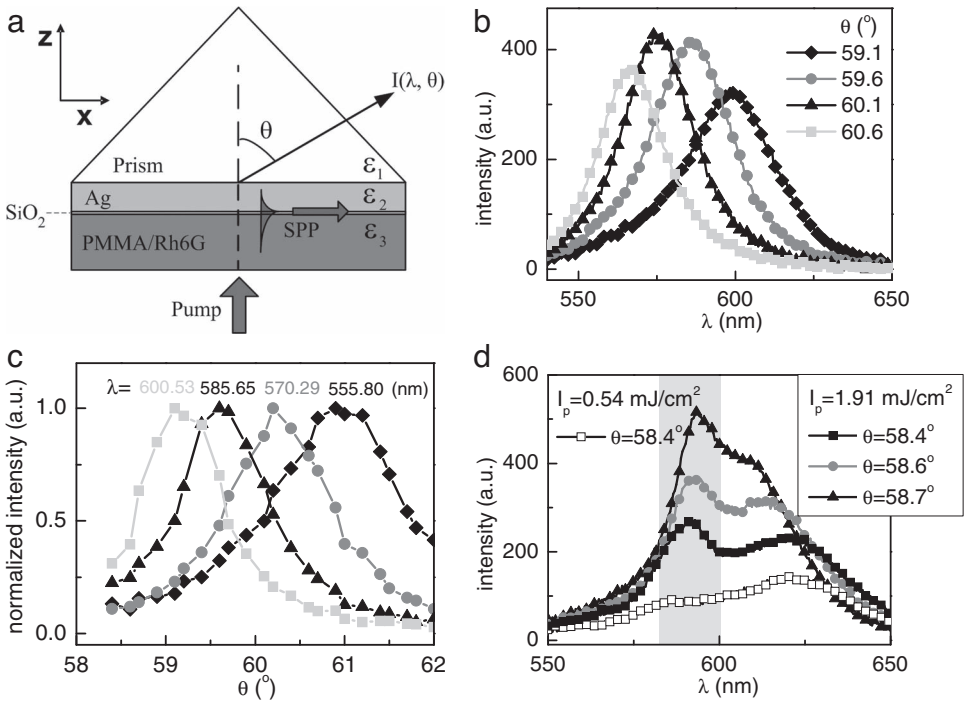

Figure 1. a) Schematic diagram of the experimental setup (further details in Experimental Section): $\varepsilon_1 = 1.846^2$ and $\varepsilon_3 = 1.5^2$. b) Decoupled emission spectra of the SPPs at different angles θ (in degrees) under a low pump intensity $I_P = 0.54$ mJ/cm^2. c) Angular distribution of SPP emission for several fixed wavelengths (as noted): $I_P = 0.54$ mJ/cm^2. d) Curves with $\theta = 58.4°$ at $I_P = 0.54$ mJ/cm^2 and $I_P = 1.91$ mJ/cm^2 indicate an emerging ASE_{SPP} peak (the ASE_{SPP} wavelength is identified at 592.87 nm), while the curves with $I_P = 1.91$ mJ/cm^2 at $\theta = 58.4°$, 58.6°, and 58.7° indicate the wavelength range of ASE as noted in gray.

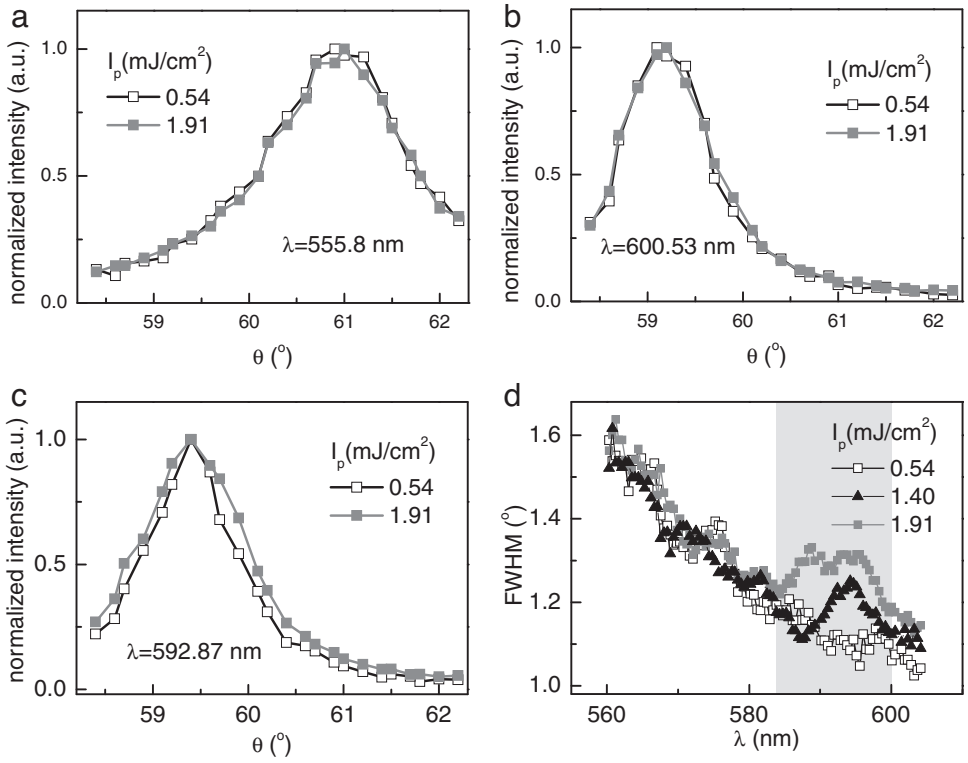

Figure 2. a–c) Angular distribution of SPP emission at 555.80, 600.53, and 592.87 nm under different I_P as noted. d) FWHM of the angular distribution of SPP emission as a function of the detection wavelength under different I_P as noted. Gray region shows the region where the FWHM is unusually increased.

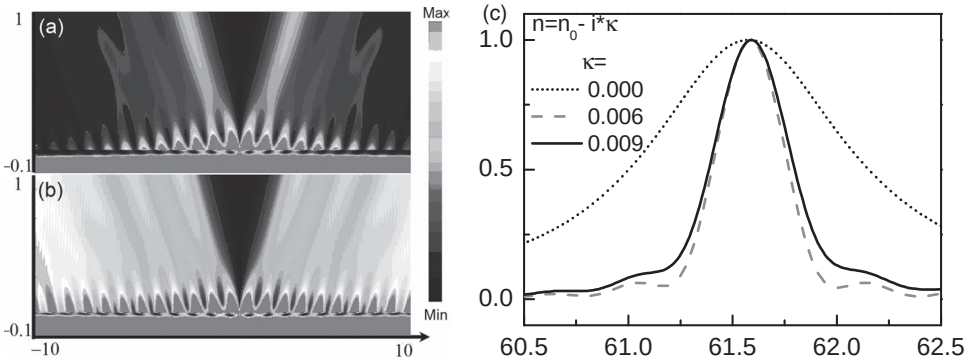

Figure 3. FDTD simulation results. Intensity distribution of the electric field near the interface of the prism and silver layer a) without and b) with gain $\kappa = 0.0085$. The *x* scale is [−10, 10] μm and the *y* scale is [−0.1, 1] μm. c) Calculated far-field angular distribution of SPP emission at 593 nm with different gain media as noted.

Firstly, at low pump intensity, the FWHM drops gradually with wavelength as an overall trend, as also indicated in Figure 1c. Secondly, it is only at the range of 582–600 nm (the gray region in Figure 2d) that the FWHM is increased with the increase of I_P. Most interestingly, the gray regions in Figure 2d and Figure 1d are almost located within the same wavelength region, i.e., the ASE_{SPP} spectral region, which implies that net gain (as manifested by the existence of ASE_{SPP}) broadens the angular distribution of SPP emission other than makes it narrower.

To verify the observed results, we simulate the experiments with the finite-difference time-domain (FDTD) method. In the simulations, an electric dipole is placed 25 nm beneath a 55-nm-thick silver film and the refractive index of the upper dielectric is set as 1.846, while the lower medium is treated as a normal medium or a gain medium (see Supporting Information (SI), Section I for details). **Figure 3**a shows the emission pattern of the dipole at wavelength 593 nm without gain, i.e., the refractive index of the lower medium is set to be 1.5. In the intensity distribution, we can see that SPP modes are excited and decoupled to radiative waves[11,12] at an angle ~60° as they propagate along the interface. Due to the intrinsic absorption and the radiative loss, the intensity of SPPs attenuates along *x* axis. When proper gain is introduced into the lower dielectric layer, for example $\kappa = 0.0085$ (the complex refractive index of the gain medium is defined as $n = n_0 - i\kappa$,[15] where κ is the imaginary part, standing for gain, and n_0 the real part), the attenuation of SPPs can be compensated and even amplified along *x* axis, as shown in Figure 3b. In our experiment, what we detect is the far-field distribution of these SPP-decoupled radiative waves. Thus we further calculate the far-field angular distribution with FDTD. The results are shown in Figure 3c, where emission peaks at ~60° can be recognized. It can be seen that the curve is narrowed at first with the increase of gain. However, as the gain continues to grow, the angular distribution is then broadened. Such a trend agrees with our experiment results and confirms our assumption that gain can induce the broadening in angular distribution of SPP emission.

To understand the underlying physics behind our observations and simulations, we further develop a theoretical model. As illustrated in **Figure 4**a, we impose an aperture $x \in [0, A]$ immediately above the upper surface of the silver film, only inside which is the electromagnetic field nonzero.[4,12] If the SPPs attenuate with propagation (the propagation length of SPPs in visible wavelength is 10–100 mm), such an aperture

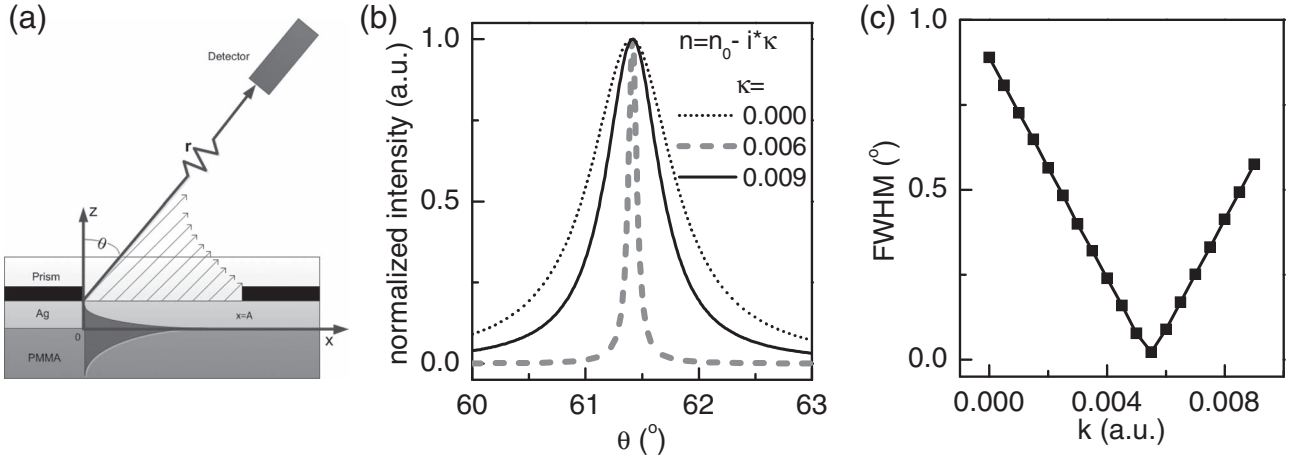

Figure 4. a) Schematic diagram of the model used in theoretical analysis. b) Calculated angular distribution of SPP emission at 593 nm with different gain media as noted. c) FWHM of the angular distribution of SPP emission as a function of gain (κ).

would not change the field distribution dramatically if A is large enough.[4,12] On the other hand, if the SPPs are amplified by the pump effects, A can be set to equal the diameter of the pump spot (1 mm),[4] which is relatively large compared with the propagation length of SPPs. Introducing such an aperture enables us to calculate the far-field distribution by using Green's theorem. Inside the prism, the SPP waves can be expressed as

$$H_y(\mathbf{r}) = Ae^{i\beta x}e^{ik_{z1}(z-a)} \quad (1)$$

where $\beta = \beta' + i\beta''$ is the SPP propagating constant determined by the sample structure,[16,17] $k_{z1} = \sqrt{\varepsilon_1 k_0^2 - \beta^2}$ with k_0 the vacuum wave number, and a is the thickness of the silver film. Using the Green theorem and integrating Equation 1 along the surface z = a, one gets the electromagnetic field of an arbitrary point in the prism

$$H_y(\mathbf{r}) = \int_{x'\in[0,\,A]} [H_y(\mathbf{r}')\cdot\nabla G(\mathbf{r}-\mathbf{r}') - G(\mathbf{r}-\mathbf{r}')\cdot\nabla H_y(\mathbf{r}')]d\mathbf{s}' \quad (2)$$

The integral is nonzero only inside the aperture $x'\in[0, A]$. By using Equation 2 to model the SPP decoupled emission in our experiment, we can deduce the electromagnetic field intensity in Fraunhofer Region (far field, see SI, Section II for details)[4,12]

$$I(r,\theta) \propto \frac{1}{(\beta' - \sqrt{\varepsilon_1}k_0\sin\theta)^2 + \beta''^2} \quad (3)$$

Starting from Equation 3 and using the optical constants of silver[18] (see SI, Section III for details), we plot the normalized curves of $I(r, \theta)$ in Figure 4b. It is seen that the evolution of the angular distribution curves is similar as those in Figure 3c.

From Equation 3, one can see that the peak position of the angular distribution curve is defined by the relation $\beta' - \sqrt{\varepsilon_1}k_0\sin\theta = 0$ while the FWHM is determined by the absolute value of β''. Whether the system is of loss or gain is determined by the sign of β''. In our structure, β'' simply contains three parts

$$\beta'' = \beta''_{\text{int}} + \beta''_{\text{rad}} + \beta''_{\text{gain}} \quad (4)$$

where β''_{int} represents the intrinsic absorption of metal (positive), β''_{rad} represents the radiative loss of the structure (positive), and the β''_{gain} is the optical gain induced by the Rh6G doped PMMA film (negative). It is known that ASE process occurs at the region where the optical gain overcomes the total loss.[7,14] Therefore in the gray region in Figure 1d and Figure 2d, there is a net gain in the structure, which means that $\beta'' < 0$. In such a region, a further increase of the pump intensity would lead to a larger absolute value of β''. As a result the FWHM is increased and dependent on I_P at the ASE_{SPP} spectral region, as shown in Figure 2d. This explains why the solid curves are broader than the dashed curves in Figure 3c and Figure 4b. On the other hand, once the investigated wavelengths are outside the ASE_{SPP} spectral region (560–582 nm) where the SPP amplification effects are weak,[10] the FWHM is simply determined by the loss in the structure ($\beta'' = \beta''_{\text{int}} + \beta''_{\text{rad}}$). As a result, the FWHM keeps unchanged when varying I_P. It is well-known that the loss in silver ($|\beta''|$) is larger at shorter wavelengths in the visible wavelength region.[18] Therefore, from Equation 3, one can expect that the FWHM is larger at shorter wavelengths, which is well manifested in Figure 2d.

With Equation 3, one can easily obtain the angular FWHM of SPP emission as a function of gain (represented by the value of κ), which is shown in Figure 4c. It can be seen that there exists an optimized value of κ to achieve a minimum FWHM. At this κ value, FWHM reaches nearly zero when the loss is completely compensated by the gain. This, from the other side, indicates the existence of the critical gain point in many other plasmonic structures, such as gain-assisted nanoparticles[15] and planar spaser structures.[19]

As pointed out in the literature,[4] the Fourier transformation of $H_y(\mathbf{r}) = Ae^{i\beta x}$ is $H(k) = \frac{1}{\pi}\frac{1}{i(\beta'-k)-\beta''}$. In such a case, one can get $I(k) \equiv |H(k)|^2 = \frac{1}{\pi^2}\frac{1}{(\beta'-k)^2+\beta''^2}$, which is of the same form as Equation 3. Therefore the measured angular distribution in our experiments (as illustrated in Figure 1c and 2a–c) is essentially the $I(k)$ versus k curves of SPPs in the Fourier space. The observed unusual angular response is thus the broadened I versus k curve in Fourier space induced by ASE_{SPP}. This, as a return, gives people a new way to recognize the SPP amplification effects in Fourier space.

It should be mentioned here that our FDTD simulation and analytical model employ a uniform distribution of gain in PMMA film by simply setting the negative imaginary part of the refractive index of the gain media, which is used to describe the experimental observations phenomenologically. In a more general situation where the pump intensity has spatial variation and the lifetime of an excited dye molecule is modified due to Purcell effect, a nonuniform spatial distribution of gain[20,21] needs to be taken into account in order to precisely describe the plasmonic problem.

In summary, we have observed the unusual angular response of ASE_{SPP} in the Kretshmann structure, i.e., the angular distribution of ASE_{SPP} is broadened with the increased gain. The observations have been further confirmed and explained by the FDTD simulations and a theoretical model respectively. However, due to the low signal-to-noise-ratio when I_P is lower than 0.54 mJ/cm^2 in our experiments, we did not observe the reduction of FWHM with increased pump intensity, which happens when β decreases from a positive value to zero. Nevertheless, the observed phenomena and theoretical studies could be helpful in understanding the interaction between gain media and plasmonic systems, and thus useful for plasmonic device designing. For example, the sensitivity of surface plasmon resonance sensor on external perturbations[22,23] is hindered by the FWHM of the reflection dip. Our studies can help to explore and design plasmonic systems for efficiently compressing the angular response of the plasmonic system[3] in order to get the optimal performance.

Experimental Section

Our experimental setup is based on a typical Kretschmann configuration.[10] As shown in Figure 1a, a prism (SF57; refractive index

NANO MICRO small

of prism, $n_{prism} = 1.846$ at wavelength 589.3 nm) is used as a substrate, and the thickness of the silver film, the SiO_2 layer, and the PMMA film is 55 nm, 5 nm, and 1.3 μm, respectively. The PMMA film ($n_{PMMA} \approx 1.5$) is doped with Rhodamine 6G dye molecules at a concentration of 0.015 mol L^{-1}. The thin SiO_2 layer is utilized to avoid the fluorescence quenching induced by direct touching of the molecules with the metal layer[24] and thus get a higher SPP excitation efficiency.[25] A laser pulse (with 532 nm wavelength, ~5 ns duration, and polarization normal to the *xz* plane) is used to excite the Rh6G molecules from the PMMA film side. Since the heat dissipation in PMMA has a characteristic time of 0.5 s,[26] we set the repetition rate of the pulse at 0.5 Hz to minimize the photodestruction. The diameter of the pump laser spot is about 1 mm, and the signals are collected by using an optical fiber (400 μm in diameter) connected to a spectrometer (Ocean Optics, USB2000). While the photonic emission of Rh6G is measured from the PMMA/Rh6G film side, the decoupled emission of SPPs are characterized from the prism side (as the arrow shown in Figure 1a), which has been utilized to identify the ASE of SPP in our previous work.[10]

Supporting Information

Supporting Information is available from the Wiley Online Library or from the author.

Acknowledgements

This work was supported by the National Key Basic Research Special Foundation of China under Grant No. 2011CB922002, and the National Natural Science Foundation of China under Grant Nos. 60736041, 11104342, and 10874238.

[1] S. A. Maier, *Plasmonics: Fundamentals and Applications* Springer, New York **2006**.
[2] J. Seidel, S. Grafstrom, L. Eng, *Phys. Rev. Lett.* **2005**, *94*, 177401.
[3] M. A. Noginov, V. A. Podolskiy, G. Zhu, M. Mayy, M. Bahoura, J. A. Adegoke, B. A. Ritzo, K. Reynolds, *Opt. Express* **2008**, *16*, 1385–1392.
[4] M. A. Noginov, G. Zhu, M. Mayy, B. A. Ritzo, N. Noginova, V. A. Podolskiy, *Phys. Rev. Lett.* **2008**, *101*, 226806.
[5] M. Ambati, S. H. Nam, E. Ulin-Avila, D. A. Genov, G. Bartal, X. Zhang, *Nano Lett.* **2008**, *8*, 3998–4001.
[6] J. Grandidier, G. C. D. Francs, S. Massenot, A. Bouhelier, L. Markey, J. C. Weeber, C. Finot, A. Dereux, *Nano Lett.* **2009**, *9*, 2935–2939.
[7] P. M. Bolger, W. Dickson, A. V. Krasavin, L. Liebscher, S. G. Hickey, D. V. Skryabin, A. V. Zayats, *Opt. Lett.* **2010**, *35*, 1197–1199.
[8] X. J. Zhang, Y. C. Li, T. Li, S. Y. Lee, C. G. Feng, L. B. Wang, T. Mei, *Opt. Lett.* **2010**, *35*, 3075–3077.
[9] D. J. Bergman, M. I. Stockman, *Phys. Rev. Lett.* **2003**, *90*, 027402.
[10] Y. H. Chen, J. F. Li, M. L. Ren, B. L. Wang, J. X. Fu, S. Y. Liu, Z. Y. Li, *Appl. Phys. Lett.* **2011**, *98*, 261912.
[11] G. W. Ford, W. H. Weber, *Phys. Rep.* **1984**, *113*, 195–287.
[12] J. Burke, G. I. Stegeman, T. Tamir, *Phys. Rev. B* **1986**, *33*, 5186–5201.
[13] J. Grandidier, G. C. Francs, S. Massenot, A. Bouhelier, L. Markey, J. C. Weeber, A. Dereux, *J. Microsc.* **2010**, *239*, 167–172.
[14] M. C. Gather, K. Meerholz, N. Danz, K. Leosson, *Nat. Photonics* **2010**, *4*, 457–461.
[15] Z. Y. Li, Y. N. Xia, *Nano Lett.* **2010**, *10*, 243–249.
[16] H. Raether, *Surface-Plasmons on Smooth and Rough Surfaces and on Gratings*, Springer-Verlag, Berlin **1988**.
[17] C. H. Liao, C. M. Lee, L. B. Chang, J. H. Tsai, *Jpn. J. Appl. Phys.* **1997**, *36*, 1105–1111.
[18] P. B. Johnson, R. W. Christy, *Phys. Rev. B.* **1972**, *6*, 4370–4379.
[19] N. I. Zheludevi, S. L. Prosvionin, N. Papasimakis, V. A. Fedotov, *Nat. Photonics* **2008**, *2*, 351–354.
[20] A. V. Krasavin, T. P. Vo, W. Dickson, P. M. Bolger, A. V. Zayats, *Nano Lett.* **2011**, *11*, 2231–2235.
[21] I. D. Leon, P. Berini, *Phys. Rew. B* **2008**, *78*, 161401.
[22] J. Homola, S. S. Yee, G. Gauglitz, *Sensor Actuat. B-Chem* **1999**, *54*, 3–15.
[23] M. Piliarik, J. Homola, *Opt. Express* **2009**, *17*, 16505–16517.
[24] O. Popov, V. Lirtsman, D. Davidov, *Appl. Phys. Lett.* **2009**, *95*, 191108.
[25] S. Hayashi, Y. Yamada, A. Maekawa, M. Fuji, *Jpn. J. Appl. Phys.* **2008**, *47*, 1152–1157.
[26] S. Popov, *Appl. Optics* **1998**, *37*, 6449–6455.

Received: September 1, 2011
Revised: December 19, 2011
Published online: February 29, 2012

